LAWRENCE
LIVERMORE
NATIONAL
LABORATORY

LLNL-TR-661658

The Watchboy Radionuclide Detector Deployment and Analysis

S. Dazeley, A. Bernstein, N. Bowden

September 30, 2014

Disclaimer

This work performed under the auspices of the U.S. Department of Energy by Lawrence Livermore National Laboratory under Contract DE-AC52-07NA27344.

The Watchboy Radionuclide Detector Deployment and Analysis

The Watchboy detector was designed to measure the rate of radionuclide production in water created via muon spallation. The three primary nuclei of interest, ^{11}Li, ^{8}He and ^{9}Li, can mimic an antineutrino induced inverse beta decay, producing a high energy beta particle in coincidence with a neutron. Their signature in Watchboy would be the passage of a muon through the target, followed some time later, characterized by the decay time of the radionuclide, by a beta and a neutron emitted in coincidence.

Watchboy was constructed between April and July 2013 at the Kimballton Underground Research Facility (KURF) in Virginia. "First light" was late in July 2013. Figure 1 shows the design of the detector hardware (not including the outer tank supporting the water). There are 16 inner target 10-inch PMTs instrumenting a volume of approximately 2 cubic meters, and 36 veto PMTs for the remaining 40 cubic meter veto volume. The veto is a volume of pure DI water surrounding the target averaging 1.4 meters thick. It serves two purposes, to indicate the passage of cosmic ray muons nearby, and to prevent fast neutrons and high energy gamma rays from the rock reaching the target. Figure 2 shows some of the installed PMTs in the outer veto and the completed inner target (left) and the bottom veto region under the target (right).

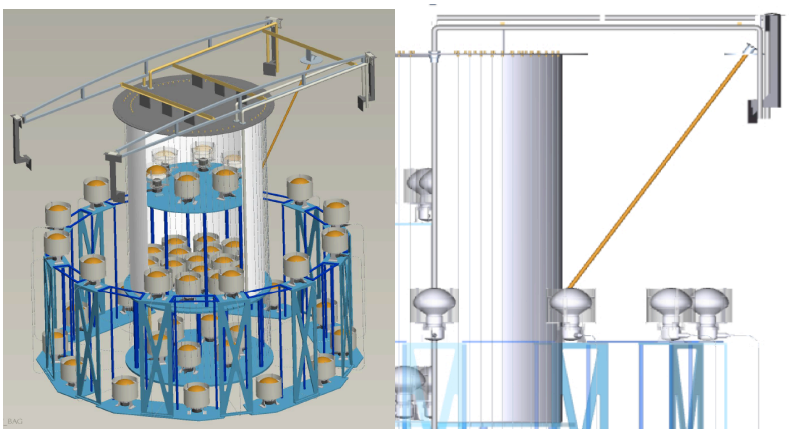

Figure 1: The Watchboy detector design inside the steel detector tank. The target gadolinium doped region containing 16 tightly packed upward facing PMTs is shown at the center of the detector (left). To the right the bag that supports the target region and the calibration source tube are shown. The source tube allows deployment of sources at the edge of the target volume.

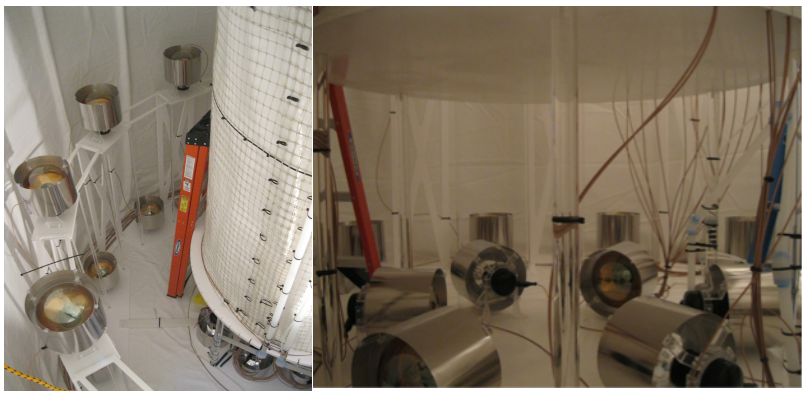

Figure 2: The outer veto PMTs are shown outside the closed inner target region (left). The lower veto PMTs are shown to the right. Note that these PMTs are horizontal and sit directly under the target.

This work was performed under the auspices of the US Department of Energy by Lawrence Livermore National Laboratory under Contract DE-AC52-07NA27344, release number LLNL-xxx-xxxxxx.

LED calibrations have been performed on a semi-regular basis to determine the PMT gains. The detector has been operational and taking physics data with correct and equalized PMT gains since August 2013.

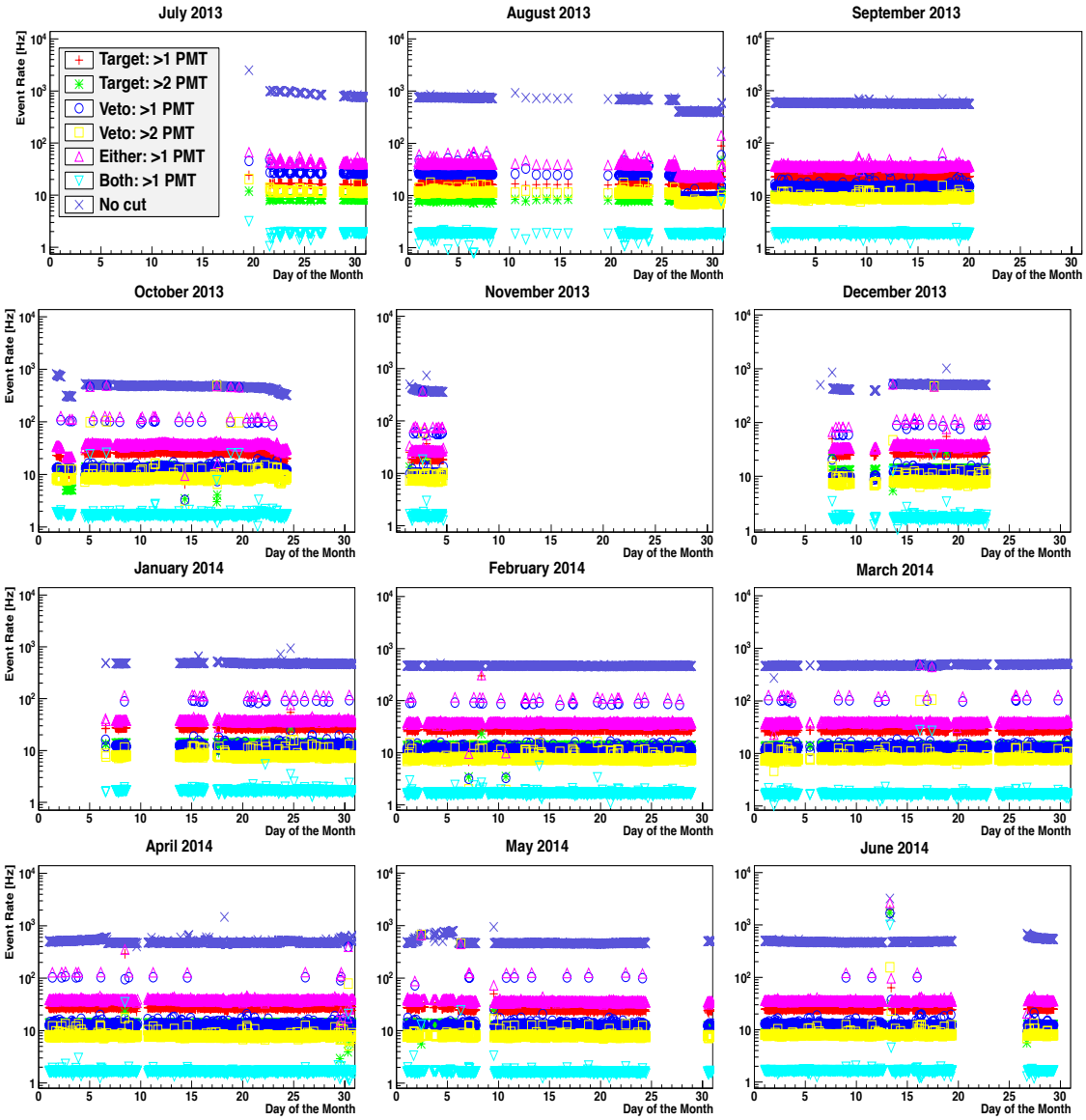

Figure 3: Event rate of the Watchboy radionuclide detector since physics running started in late July 2013. The event types shown are 1) raw event rate, 2) two or more PMTs in target, 3) two or more PMTs in veto, 4) three or more PMTs in target, 5) three or more PMTs in veto, 6) two or more PMTs in either, 7) two or more PMTs in both.

Data Taking and Analysis

The hardware trigger is very simple. The target region PMTs are grouped into four groups of four. The veto PMTs are grouped into groups of either four or three. In some regions, such as the top veto, there are only six PMTs, so groups of three were optimal. The analogue sum from each group is monitored on a continuous basis. If any single group produces a signal greater than the group threshold (a few photoelectrons), the whole detector is triggered and all 52 PMT signals are digitized and read out to disk. Figure 3 shows the event rate in both the target and veto regions for a variety of

This work was performed under the auspices of the US Department of Energy by Lawrence Livermore National Laboratory under Contract DE-AC52-07NA27344, release number LLNL-xxx-xxxxxx.

event types. The most common event trigger type is attributed to single PMT noise triggers – as shown in the figure. These are mostly PMT after pulsing events, or similar electronic/noise non-physics events.

PMT signals from each event are digitized by four 16-channel Struck SIS3316-250-14 digitizers. Two primary DAQ modes are possible – full 128 sample waveforms at 4 nanoseconds per waveform, or a set of eight integrated waveform sections. Watchboy employs the integrated waveform approach during normal physics data taking as the waveform shapes are expected to yield little relevant physics information in a Cherenkov detector. **Figure 4** shows an example of a hypothetical waveform at Watchboy. The integrated waveform sections are divided as shown. The timing between the trigger and the initiation of each waveform is tuned so that the PMT signal generally falls between sample #32 and 62. We use samples 0 to 32 for a determination of the pedestal.

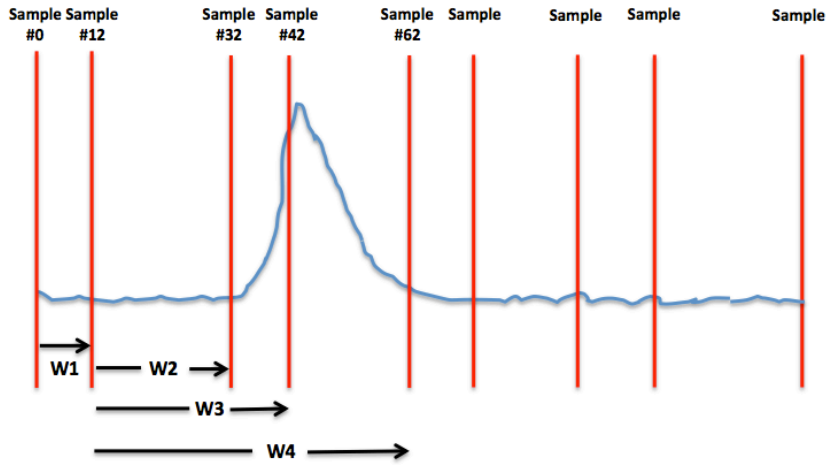

Figure 4: The Watchboy PMT signal digitization is a set of eight integrated sections of a 128 sample waveform recorded from all 52 PMT channels every time the detector is triggered. The first four integration sections from the target are shown (W1 through W4). Each sample corresponds to 4 nanoseconds.

Single photoelectron (SPE) calibration runs are performed approximately every three months using green LEDs judiciously placed in each of the detector volumes. When biased so that ~10% of the PMTs detect a photon per pulse, two histogram peaks are generated (pedestal and single photoelectron), providing the needed ADC to photoelectron conversion ratios. The first step in the analysis is to equalize the PMT gains and convert all the PMT signals in each event to "detected photoelectrons" using a recent calibration run.

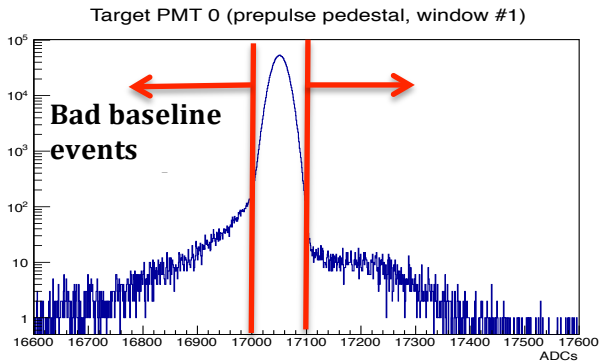

Figure 5: A histogram of the pedestal W1 values from PMT #0 in the target built up over the course of a one hour physics data run. The pedestal value is given by the mean of the Gaussian fit to the central peak. Most events fall within 4 sigma of the pedestal (red lines). Events that fall outside this range are assumed to be bad due to baseline variation – which sometimes follows from an energetic preceding event.

This work was performed under the auspices of the US Department of Energy by Lawrence Livermore National Laboratory under Contract DE-AC52-07NA27344, release number LLNL-xxx-xxxxxx.

Events with an unstable waveform baseline are then removed. A histogram of the pedestal integration window W1 is shown in Figure 5 for a one-hour regular physics run. After fitting a Gaussian curve to the pedestal peak, events with any single PMT W1 signal 4σ greater than or less than the Gaussian mean are identified and removed.

PMT afterpulsing causes a significant fraction of event triggers in Watchboy. In most cases only a single PMT contributes to the total event signal. We identify these events on the basis of their "charge balance", defined (in the 16 PMT target) as

$$\boldsymbol{charge\ balance} = \sqrt{\frac{\sum_i \boldsymbol{Q_i^2}}{\boldsymbol{Q_{sum} Q_{sum}}} - \frac{\mathbf{1}}{\mathbf{16}}}$$

where Q_i is the charge of the *ith* PMT and Q_{sum} the total event charge. If the total event signal is distributed approximately evenly among all the PMTs in a detector region, the resulting charge balance asymptotes towards *0*. Alternatively, if most of the signal is in a single PMT the resulting value is close to *1.* Since the walls of the detector are highly reflective, real physics events tend to produce Cherenkov light that bounces around the detector volume a number of times before being detected. The result is a relatively even distribution of signal among the PMTs. **Figure 6** shows the distribution of detector response and charge balance for a set of regular DAQ events and a 0.2 µCi ^{252}Cf calibration run. The 252Cf run is relevant here because most events are genuine neutron captures with small charge balance. **Figure 3** also illustrates the large fraction of events (~90%) dominated by single PMTs.

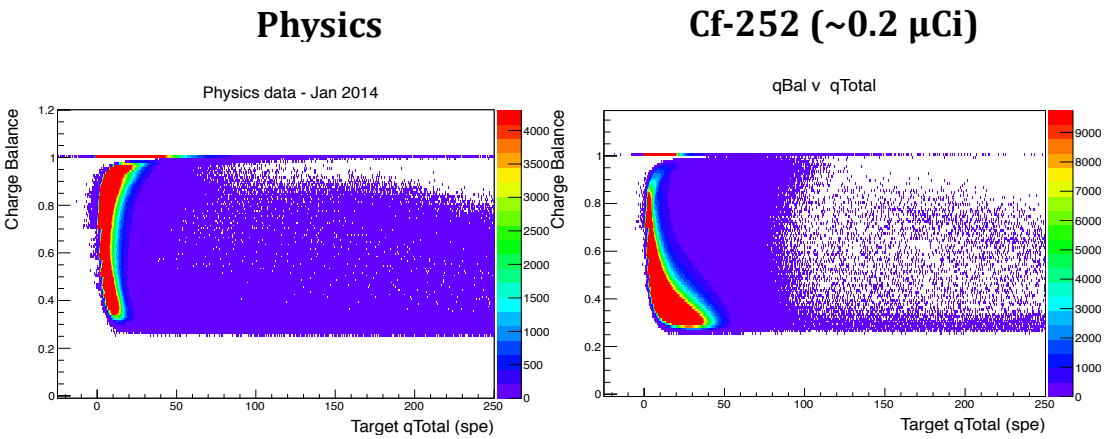

Figure 6: Scatter plots of regular physics events (left) and neutron rich ^{252}Cf events (right). The charge balance parameter is plotted as a function of the total number of photoelectrons detected in the target.

A ^{252}Cf source calibration every few months is used to produce high concentrations of neutron capture events at will in the target, which we then use to tune our simulation and define the characteristics of neutron capture in the detector (an important signature of ^{9}Li, ^{8}He and ^{11}Li). **Figure 7** compares regular physics data to a ^{252}Cf data run in separate plots of total event charge and charge balance. The ^{252}Cf neutron captures are primarily concentrated in a zone between ~20 and ~100 photoelectrons, with small charge balance.

This work was performed under the auspices of the US Department of Energy by Lawrence Livermore National Laboratory under Contract DE-AC52-07NA27344, release number LLNL-xxx-xxxxxx.

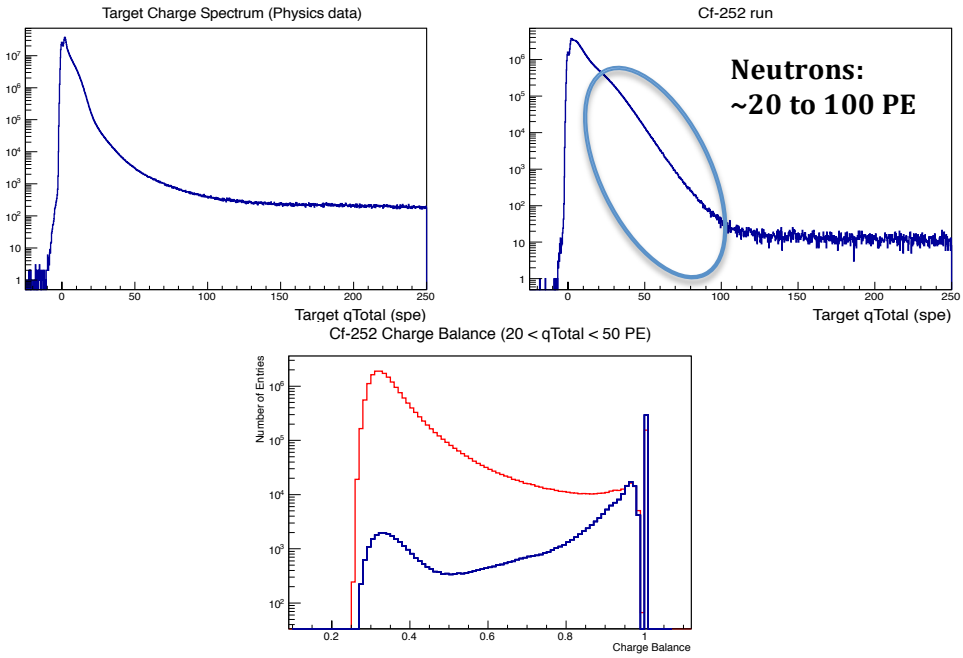

Figure 7: The total number of photoelectrons detected in the target from a regular physics run and a ^{252}Cf calibration run (top). Below, a comparison of the charge balance for neutron like events from a ^{252}Cf run (red) compared to a regular physics run (dark blue). "Neutron-like" here refers to target events producing between 20 and 100 photoelectrons.

As stated earlier, the Watchboy detector was designed to detect radionuclides created via muon spallation in water. The analysis searches for a telltale exponential lifetime characteristic of each nuclei of interest. Since ^{8}He and ^{9}Li have long lifetimes (172 and 256 milliseconds respectively), in order to see these exponentials over background, the muon rate should be no higher than ~1Hz. Muon rates significantly lower than ~1Hz will impact the rate of radionuclide production in the target, higher and it will be impossible to discriminate between the signal and background. **Figure 8** shows the time distribution of muons in the target for the month of January. Muons were identified as having a total event charge greater than 100 photoelectrons – the approximate upper limit detector response to a neutron capture (see **Figure 7**).

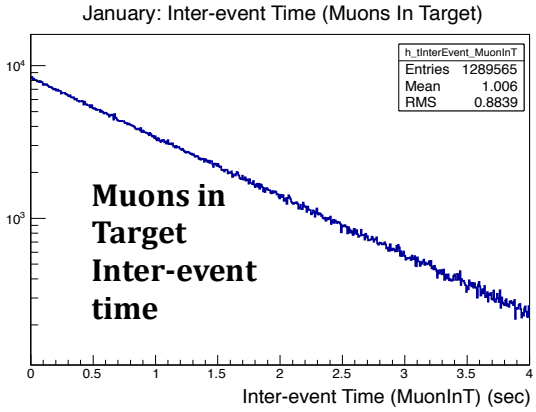

Figure 8: The time between successive muons in the Watchboy target volume.

The muon time distribution follows an exponential with mean inter event time of 1.1 seconds (.9 Hz), an ideal muon rate for this experiment.

This work was performed under the auspices of the US Department of Energy by Lawrence Livermore National Laboratory under Contract DE-AC52-07NA27344, release number LLNL-xxx-xxxxxx.

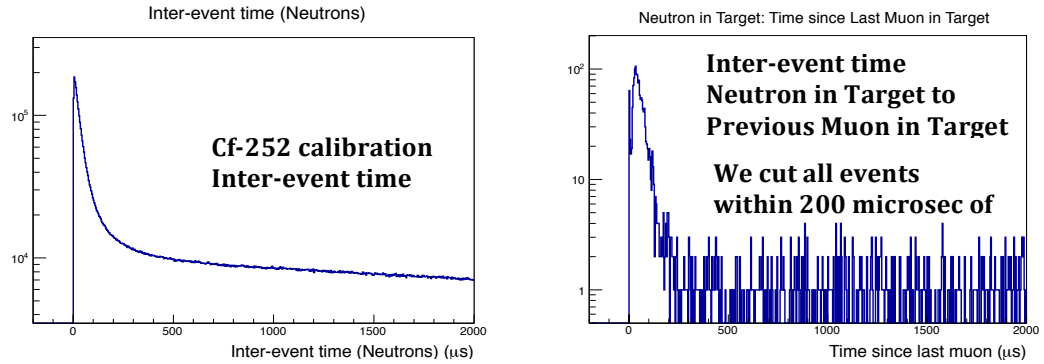

Figure 9: The time between successive neutron-like events during a ^{252}Cf calibration run (left). Note there is both a correlated component and an uncorrelated component. The time to the previous veto muon given the detection of a neutron-like event in the target (right).

Figure 9 shows the inter event time distribution for a selection of neutron-like events, taken from a ^{252}Cf calibration run. We find at least two event-types of interest – correlated and uncorrelated neutrons. Most correlated pairs are detected within ~200 microseconds. However, there is a small population that extends out to over 500 microseconds. Simulations show that these events occur when a neutron thermalizes close to, but just outside the target. From previous hydrogenous experiments such as KamLAND and Super-K, we expect the neutron capture time in the deionized veto to be ~200 microseconds. It may be possible for some neutrons to survive for up to a millisecond before being captured. Since muon induced neutron production is a background for Watchboy in the physics analysis, all events within one millisecond of a muon in the veto or target are vetoed. Since the muon rate is very low the dead time as a result of this cut is very small. In **Figure 9** (right) the time to next event following a muon in either the veto or target before the veto is applied. A population of correlated neutrons can be easily identified below about 200 microseconds.

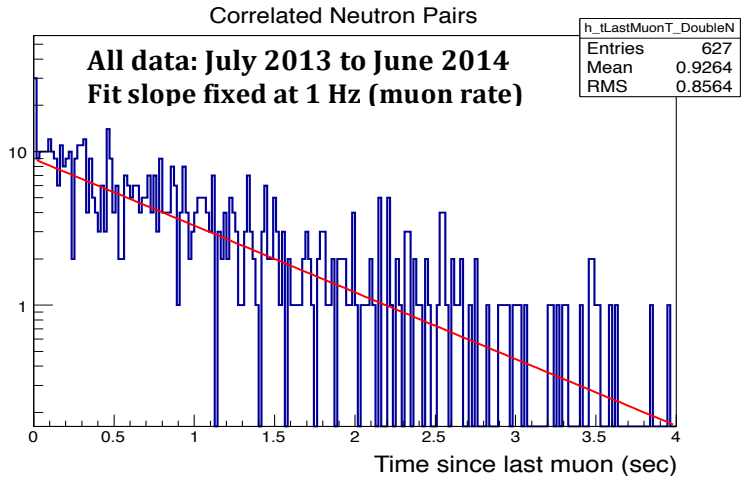

Figure 10: After 221 live days, 627 correlated neutron pairs have been detected in the target. Plot here for each of these pairs are the distribution of times to the previous muon through the target.

After applying the millisecond muon veto cut, we searched for correlated neutron-like event pairs (two neutron–like events within 200 milliseconds). In **Figure 10** we plot them as a function of the time to the previous muon. Ultimately, the radionuclide analysis will search for pairs of correlated events – a high-energy beta followed by a neutron capture. A simulation, tuned to reproduce the

This work was performed under the auspices of the US Department of Energy by Lawrence Livermore National Laboratory under Contract DE-AC52-07NA27344, release number LLNL-xxx-xxxxxx.

^{252}Cf calibration, will be used to predict the detector response for these events. The application of the final analysis cuts awaits the results of this simulation.

The Simulation

A GEANT4 simulation of the Watchboy detector has been constructed in order to predict the likely detector response to events of interest, such as ^{9}Li, ^{8}He and ^{11}Li. In order to verify that the simulation is an accurate model of the detector, we test if it reproduces the results of the ^{252}Cf calibration runs. The detector volume dimensions were taken directly from the Watchboy design. The three primary unknown detector characteristics that cannot easily be measured are the water attenuation length, wall reflectivity and the PMT quantum efficiency. We assumed that the wall reflectivity and water attenuation length act together to effectively reduce the number of times photons can bounce around the target volume before being detected. The wall reflectivity is also assumed to be relatively constant over the whole data-taking period, whereas water attenuation is expected to deteriorate slowly over time. For these reasons we make a simplifying assumption – that we can model most detector target conditions effectively by setting the wall reflectivity to a reasonable and constant average value (90%), and we can tune the water attenuation to reproduce our calibrations.

The ^{252}Cf calibration source location is at the end of a long tube on the edge of the target, about 50cm above the target PMTs (see **Figure 1**, the calibration tube is shown in orange). Source neutrons which penetrate the target mostly capture on gadolinium near the edge. The resulting Cherenkov light primarily falls upon the target PMTs situated closest to the source. This effect is observed in simulation. By splitting the 16 target PMTs into two groups of eight based on how many total photoelectrons they detect, we can obtain the ratio 8_low/8_high. This ratio is sensitive to the water attenuation, but completely insensitive to the average PMT quantum efficiency. **Figure 11** shows a surface plot of the 8_low/8_high ratio as a function of both parameters.

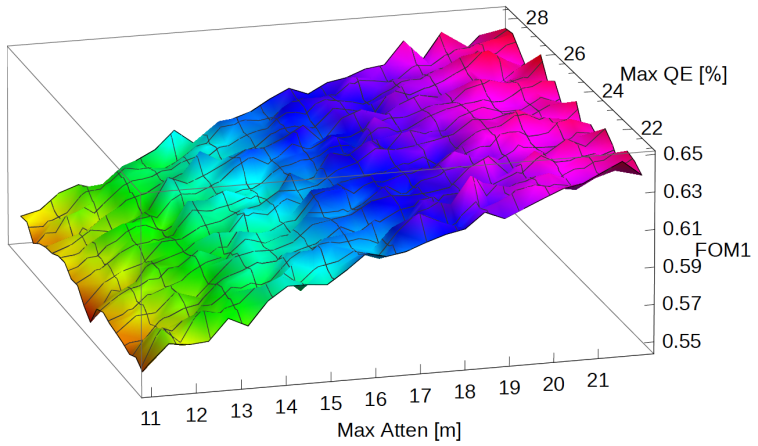

Figure 11: The value of 8_low/8_high (see text for definition), as a function of quantum efficiency and water attenuation length. 8_low/8high should asymptote towards unity if water attenuation is infinite (since Cherenkov photons will not be limited in range within the detector. Note that the 8_low/8_high is not sensitive to variations in quantum efficiency.

The 8_low/8_high values obtained from ^{252}Cf calibrations vary between 0.62 and 0.66. Since we lack a measurement of PMT to PMT quantum efficiency variation, we do not place too much weight on this comparison. Nevertheless, we do use it as an approximate guide for simulation tuning. **Figure 11** indicates the water attenuation is likely to be somewhere in the range 10 to 25 meters.

This work was performed under the auspices of the US Department of Energy by Lawrence Livermore National Laboratory under Contract DE-AC52-07NA27344, release number LLNL-xxx-xxxxxx.

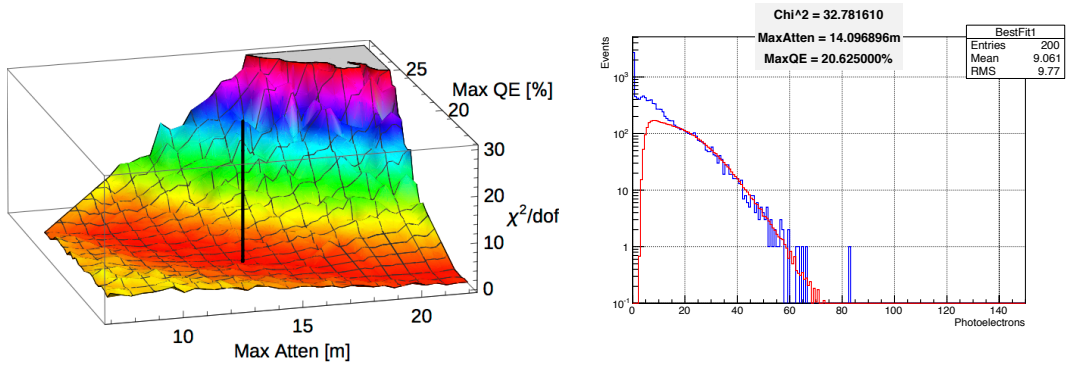

Figure 12: Simulations of neutron capture were compared to ^{252}Cf calibrations for a number of independent simulations at different PMT quantum efficiencies and water attenuation lengths. A χ^2 value corresponding to the fit was evaluated at each grid point and plotted (left). The best fit between real data and simulation is shown at attenuation length 14.1 meters and maximum quantum efficiency 20.6 %.

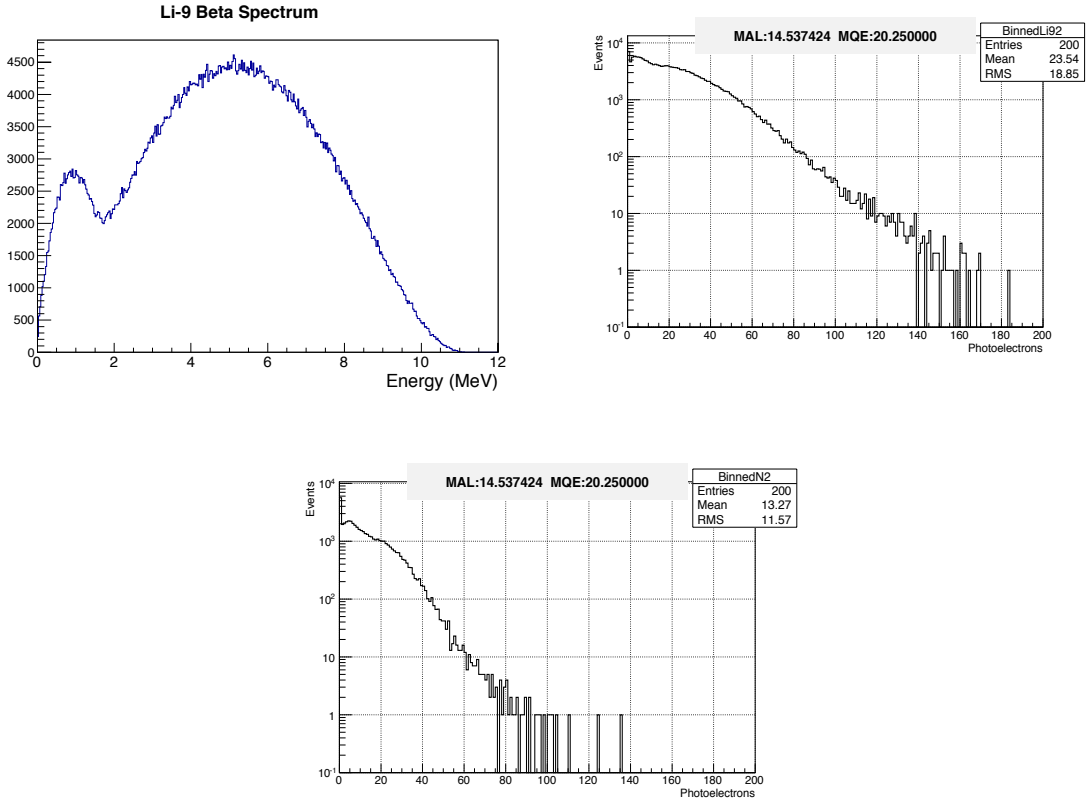

Figure 13: The ^{9}Li energy spectrum used as input to the simulation (left top). ^{9}Li was simulated isotropically throughout the target volume to determine the detector response. The resulting ^{9}Li detector response in terms of detected photoelectrons is shown (right top). The neutron capture detector response is shown below.

The primary method for tuning the simulation is to compare the real detector response to ^{252}Cf neutron captures with the corresponding predicted detector response from the simulation. We tested a range of water attenuation lengths and quantum efficiencies as shown in **Figure 12**. For each pair of inputs a simple χ^2 test was performed over a limited number of bins (57 bins between

This work was performed under the auspices of the US Department of Energy by Lawrence Livermore National Laboratory under Contract DE-AC52-07NA27344, release number LLNL-xxx-xxxxxx.

18pe and 60pe), assuming Gaussian statistics. An example of the best fit is shown also in **Figure 12**, and a surface plot of χ^2 values over the nearby parameter space. A preferred band of QE and attenuation length appears as a valley in the χ^2 test. The best fit was at 14 meters attenuation length and QE 20.6%. **Figure 13** shows the simulated detector response to a selection of isotropically distributed ^{9}Li beta prompts and neutron captures throughout the target. The input beta energy spectrum is also shown.

This work was performed under the auspices of the US Department of Energy by Lawrence Livermore National Laboratory under Contract DE-AC52-07NA27344, release number LLNL-xxx-xxxxxx.